OPEN

Original article

Nuclear Medicine Communications

Pilot study of ^{68}Ga-DOTA-F(ab′)$_2$-trastuzumab in patients with breast cancer

Volkan Beylergil[a], Patrick G. Morris[b], Peter M. Smith-Jones[a], Shanu Modi[b,g], David Solit[c], Clifford A. Hudis[b,g], Yang Lu[a], Joseph O'Donoghue[d], Serge K. Lyashchenko[e], Jorge A. Carrasquillo[a,f], Steven M. Larson[a,f] and Timothy J. Akhurst[a,f]

Objective **^{68}Ga-1,4,7,10-Tetraazacyclododecane-*N*,*N*′,*N*″,*N*‴-tetraacetic acid (DOTA)-F(ab′)$_2$-trastuzumab [^{68}Ga-DOTA-F(ab′)$_2$-trastuzumab] has been developed at our institution as a positron imaging reagent for assessing human epidermal growth factor receptor 2 (HER2) expression status by in-vivo imaging. Initial studies on animals demonstrated promising results in the monitoring of treatment response to heat shock protein 90-targeted drugs that inhibit the client protein HER2. We report here our initial clinical experience in the assessment of the toxicity, pharmacokinetics, biodistribution, and dosimetry profile of ^{68}Ga-DOTA-F(ab′)$_2$-trastuzumab with PET/computed tomography using a mean of 236 MBq/5 mg administered intravenously.**

Materials and methods **A group of 16 women with breast cancer were enrolled in this study. The one patient who did not receive ^{68}Ga-DOTA-F(ab′)$_2$-trastuzumab was excluded from analysis. Both HER2-negative ($n=7$) and HER2-positive ($n=8$) cases were studied. Among the latter, seven had undergone trastuzumab treatment previously and one had not.**

Results **It was determined that ^{68}Ga-DOTA-F(ab′)$_2$-trastuzumab was well tolerated, with a $T_{½}$ of $\sim$3.6±0.9 h; the critical organ was the kidney, with a mean dose of 0.383 cGy/37 MBq; and tumor targeting was seen in 4/8 patients with HER2-positive disease.**

Conclusion **The reagent is safe, and assessments through additional studies in a better-defined group of patients, using larger administered masses of antibodies, with a better immunoreactive fraction are needed.** ***Nucl Med Commun*** **34:1157–1165 © 2013 Wolters Kluwer Health | Lippincott Williams & Wilkins.**

Nuclear Medicine Communications 2013, **34:**1157–1165

Keywords: breast cancer, F(ab′)$_2$-trastuzumab, ^{68}Ga, Herceptin, PET/CT

[a]Department of Radiology, Molecular Imaging and Therapy Service, [b]Department of Medicine, Breast Cancer Medicine Service, [c]Human Oncology and Pathogenesis Program, [d]Department of Medical Physics, [e]Radiochemistry and Molecular Imaging Probes Core Facility, Memorial Sloan-Kettering Cancer Center, Departments of [f]Radiology and [g]Medicine, Weill Cornell Medical College, New York, New York, USA

Correspondence to Volkan Beylergil, MD, Molecular Imaging and Therapy Service, Box 77, Memorial Sloan-Kettering Cancer Center, 1275 York Avenue, New York, NY 10065, USA
Tel: +1 212 639 7372; fax: +1 212 717 3263; e-mail: beylergv@mskcc.org

Present address: Peter M. Smith-Jones: Department of Radiology, University of Colorado Denver, Denver, Colorado, USA

Present address: Timothy J. Akhurst: Department of Nuclear Medicine, Peter MacCallum Cancer Centre, East Melbourne, Victoria, Australia

Present address: Yang Lu: Department of Radiology, University of Illinois Hospital and Health Science System, Chicago, Illinois, USA

Received 13 May 2013 **Accepted** 15 August 2013

Introduction

Human epidermal growth factor receptor 2 (HER2) is a transmembrane receptor in the HER family of receptor tyrosine kinases that is overexpressed in $\sim$25% of patients with breast cancer, with effects on the regulation of cell growth, survival, differentiation, angiogenesis, and DNA repair [1,2]. As HER2 has a pathophysiological role, it has been a target for therapeutic interventions with both monoclonal antibodies such as trastuzumab and small-molecule tyrosine kinase inhibitors [3]. Although the use of trastuzumab is associated with a survival benefit, tumors will often develop resistance; thus, new approaches for targeting this pathway are being actively investigated [3,4]. Radiolabeled trastuzumab offers the potential of optimization/rationalization of therapy in an individual patient. If HER2 status can be accurately assessed noninvasively, imaging might be used to stratify the number and distribution of HER2-positive tumors, which could be particularly useful given the challenges of clinical HER2 testing in some patients [5]. This could theoretically allow improved selection of therapies for patients with HER2-positive breast cancer. It is also possible that a noninvasive test might identify HER2-positive clones within the many metastases of an otherwise HER2-negative tumor and that targeted therapy might then be useful.

0143-3636 © 2013 Wolters Kluwer Health | Lippincott Williams & Wilkins

DOI: 10.1097/MNM.0b013e328365d99b

Several studies have utilized radiolabeled intact trastuzumab for targeting HER2 in the preclinical or clinical setting [6–11]. Because of the kinetics of intact immunoglobulin G (IgG), initial studies with trastuzumab utilized isotopes with long half-lives, such as ^{111}In, and more recently ^{89}Zr, to take advantage of the higher sensitivity and resolution of PET [10–12]. Although these radionuclides have been shown to target HER2 *in vivo*, their long half-lives of 67.4 and 78 h are suboptimal for performing repeated pharmacodynamic studies.

We have generated and labeled an F(ab′)$_2$ fragment of trastuzumab with ^{68}Ga, a short-lived, 68 min half-life positron emitter, which allows the sequential noninvasive quantitation of HER2 expression using PET imaging. Using this reagent we have developed a method for imaging the downstream effects of inhibition of heat shock protein 90 (HSP90) by 17-*N*-allylamino-17-demethoxygeldanamycin (17-AAG) [13]. This method allowed us to noninvasively image the pharmacodynamics of a targeted drug and facilitate the rational design of combination therapy based on target inhibition.

In this study we used this same ^{68}Ga-1,4,7,10-tetraazacyclododecane-*N*,*N*′,*N*″,*N*‴-tetraacetic acid (DOTA)-F(ab′)$_2$-trastuzumab [^{68}Ga-DOTA-F(ab′)$_2$-trastuzumab] reagent to assess its safety, feasibility, biodistribution, tumor targeting potential, dosimetry, and pharmacokinetics in women with metastatic or unresected breast cancer.

Materials and methods

Synthesis of ^{68}Ga-DOTA-F(ab′)$_2$-trastuzumab

Production of ^{68}Ga

^{68}Ga was eluted from a 50 mCi ^{68}Ga/^{68}Ge generator (Cyclotron Co. Ltd, Obninsk, Russia). The generator was eluted with 0.1 mol/l hydrochloric acid as per the manufacturer's instructions. ^{68}Ga was assayed with a dose calibrator. The ^{68}Ge content was determined after waiting 48 h for the ^{68}Ga to decay and then counting with a Na(Tl)I detector, together with a calibrated source of ^{68}Ge. The measured mean ^{68}Ge breakthrough in the product was measured at a mean of 125 nCi (range 56–240 nCi).

F(ab′)$_2$-trastuzumab patient dose

Trastuzumab (Herceptin; Genentech, South San Francisco, California, USA) was purchased as a lyophilized white powder, reconstituted with the supplied solvent, and digested using pepsin immobilized on agarose beads. Briefly, 1.3 g of trastuzumab was repeatedly diluted with 20 mmol/l sodium acetate buffer (pH 4.5) and concentrated using a stirred cell concentrator equipped with a 30 kDa cutoff membrane. To generate F(ab′)$_2$, the antibody was then gently shaken overnight with 5 ml of immobilized pepsin (Pierce Biotechnology, Rockford, Illinois, USA) in 100 ml of sodium acetate buffer. The protein was recovered by centrifugation and the supernatant buffer exchanged with 50 mmol/l sodium phosphate (pH 7.1) and concentrated to 100 ml using the stirred cell equipped with a 30 kDa cutoff membrane. Intact IgG and any remaining Fc portions were removed using a 2 × 5 ml protein A column (Pierce Biotechnology).

DOTA-F(ab′)$_2$-trastuzumab production

F(ab′)$_2$-trastuzumab was conjugated with 1,4,7,10-tetraazacyclododecane-*N*,*N*′,*N*″,*N*‴-tetraacetic acid (DOTA). Briefly, 625 mg of DOTA (Simafex, Marans, France) and 137 mg of *N*-hydroxysuccinimide (Sigma-Aldrich, St Louis, Missouri, USA) were dissolved in water and the pH was adjusted to 7.2 with NaOH. This mixture was cooled on ice for 30 min and 125 mg 1-ethyl-3-(3-dimethylaminopropyl)-carbodiimide (Sigma-Aldrich) was then added to it. This reaction mixture was cooled on ice for 1 h and added to 0.5 g of F(ab′)$_2$-trastuzumab in 50 ml of 50 mmol/l sodium phosphate (pH 7.3). The resultant DOTA-F(ab′)$_2$-trastuzumab was separated from the excess DOTA and other reactants by repeated washing with 1.0 mol/l NH_4OAc (20 ×) and ultrafiltration concentration. The final vialed product had 4.9 DOTA per antibody fragment. The number of DOTA moieties per antibody fragment was determined according to the method described by Smith-Jones and Solit [14]. The purified conjugate was then sterilized by filtration through a 0.22 μm filter and stored in sterile polypropylene vials at 2–8°C as 5 mg/0.5 ml 1 mol/l NH_4OAc.

Radiolabeling

DOTA-F(ab′)$_2$-trastuzumab was labeled with ^{68}Ga. In brief, 15.7–40.7 mCi (mean 27.9 mCi) ^{68}Ga eluted from the generator was incubated with 0.5 ml of DOTA-F(ab′)$_2$-trastuzumab (10 mg/ml in 1 mol/l NH_4OAc) and the solution was incubated at 37°C for 15 min. The reaction mixture was quenched with 100 μl of 5 mmol/l diethylenetriaminepentaacetic acid (DTPA) (pH 7.0) for 5 min at 37°C and then separated on a 20 ml Biogel P-6 column (Bio-Rad, Hercules, California, USA) equilibrated with 1% human serum albumin (HSA) in 0.9% NaCl. The column was eluted with 1% HSA in 0.9% NaCl and the purified ^{68}Ga-DOTA-F(ab′)$_2$-trastuzumab was sterile-filtered and diluted to 5 ml with 1% HSA in 0.9% NaCl. Patients received a net mean administered activity of 236 MBq (range 126–309 MBq) and 4.5–5.5 mg ^{68}Ga-DOTA-F(ab′)$_2$-trastuzumab at the time of injection.

Quality control

The amount of nonprotein ^{68}Ga in radiolabeled F(ab′)$_2$-trastuzumab preparations was evaluated using instant thin-layer chromatography and was less than 10% (the mean value for all 15 patients was 3.2%). It was ascertained with silica gel-impregnated glass fiber strips and 5 mmol/l DTPA (pH 7.0). The antibody complex

and bound Ga^{3+} remained at the origin, and free Ga^{3+} moved with the solvent front as a DTPA complex.

The median immunoreactivity of ^{68}Ga DOTA-F(ab′)$_2$-trastuzumab was 51.3%. Immunoreactivity experiments were carried out using serial dilutions of HER2-expressing BT-474 cells according to the method described by Lindmo *et al.* [15]. This method extrapolates the binding of the radiolabeled antibody at an infinite excess antigen. Test solutions containing about 20 000 cpm of radiolabeled DOTA-F(ab′)$_2$-trastuzumab and increasing amounts of BT-474 breast cancer cells were incubated at ambient temperature before being isolated (by centrifugation) and washed with ice-cold PBS. The cells were then counted in a gamma counter with standards representing the total radioactivity added. The data were then plotted using the Lindmo method as the reciprocal of the substrate concentration (*X*-axis) against the reciprocal of the fraction bound (*Y*-axis). The data were then fitted according to a least-squares linear regression method; the *y*-intercept gives the reciprocal of the immunoreactivity.

Study population and inclusion criteria

A total of 16 female patients (median age 55, range 39–75) were enrolled in this single-arm, prospective, nonblinded trial. The one patient who did not receive ^{68}Ga-F(ab′)$_2$-trastuzumab was excluded from the analysis. The patient and tumor characteristics are shown in Table 1. This study was performed under an investigational new drug application and was approved by the Institutional Review Board. All patients gave written informed consent. Inclusion criteria included age greater than or equal to 18 years, presence of measurable or evaluable breast cancer, and a Karnofsky performance score of at least 60. Patients were required to have a platelet level of 75 k/mcl or higher; an absolute neutrophil count of 1.5 k/mcl or higher; a white blood cell count of 3.0 k/mcl or higher; a bilirubin level of 2.5 mg/dl or lower; and a creatinine level of 2.0 mg/dl or lower. In addition, patients were required to have no clinically significant heart disease. All patients underwent a fluorine-18 fluorodeoxyglucose (^{18}F-FDG) PET/computed tomography (CT) scan within 4 weeks.

Antibody administration, pharmacokinetics, and imaging

The antibody was administered intravenously in 5–15 ml 5% HSA in less than 5 min using an inline (0.22 μm) filter, followed by a flush of 15 ml of 5% HSA. The residual activity was measured and the net administered dose was determined. A separate intravenous line was used for blood sampling before administration of ^{68}Ga-DOTA-F(ab′)$_2$-trastuzumab and at ~5, 10, 30, and 60 min and 3–6 h after infusion. Blood samples were centrifuged and aliquots of serum were counted in duplicate in a well counter, together with a known standard. The activity was expressed as %ID/l. Time–activity data were fitted to a single and biexponential function using GraphPad Prism V5.03 (GraphPad Software, San Diego, California, USA). In all but two cases the data were best fitted by a single exponential clearance; thus, these parameters were used to determine the half-life, concentration in the central compartment at T_0 (C_0), volume of the central compartment, area underneath the curve, and clearance.

To determine the accuracy of PET to quantitate ^{68}Ga activity, the %ID/l in the blood, based on maximum and mean standardized uptake value (SUV_{max} and SUV_{mean})

Table 1 Patient characteristics and visual analysis

Patient number	Tumor histology	HER2 status	Method	Trastuzumab (last dose)	Treatment at the time of ^{68}Ga	Positive sites on ^{18}F-FDG PET/CT	Positive sites on ^{68}Ga trastuzumab
1	Invasive ductal	Positive	FISH	28 days ago	Tras + letrozole	Breast, axilla, LNs, multiple bones	Positive lytic skull lesion
2	Invasive ductal	Positive	FISH	5 months ago	Vinorelbine	Multiple liver, lung, and bones	Minimal uptake in lung lesions
3	Invasive ductal	Positive	FISH	2 months ago	Letrozole	>20 brain mets and multiple bones	None
4	Breast cancer NOS	Positive	FISH	3 months ago	CAPE	Liver, right adrenal, and LNs	None
5	Invasive ductal	Positive	IHC	8 days ago	Tras + letrozole	Multiple bone lesions	None
6	Breast cancer NOS	Positive	IHC	5 months ago	Lapatinib	Left adrenal, hilar LN, and bone	None
8	Invasive ductal	Negative	IHC	NA	Irinotecan	Multiple bone lesions, LNs	None
9	Invasive ductal	Negative	FISH	NA	Etoposide	Liver, multiple bone, and LNs	None
10	Invasive ductal	Negative	FISH	NA	CAPE	LNs including right internal mammary	None
11	Invasive ductal	Negative	IHC	NA	CAPE + BEV	Multiple bone lesions and LNs	None
12	Invasive lobular	Negative	IHC	NA	Fulvestrant	Multiple bone lesions	None
13	Invasive ductal	Negative	FISH	NA	CAPE	Liver (diffuse) and multiple bones	None
14	Invasive ductal	Negative	IHC	NA	Paclitaxel + BEV	Liver, lungs, and multiple bones	None
16	Invasive ductal	Positive	FISH	2 days ago	Tras + CAPE	Brain (left postcentral gyrus) and LN	Uptake in the brain lesion
17	Invasive ductal	Positive	IHC	NA	None (preoperative)	Right breast (primary) and axilla LN	Minimal uptake in the primary tumor

BEV, bevacizumab; CAPE, capecitabine; CT, computed tomography; ^{18}F-FDG, fluorine-18 fluorodeoxyglucose; FISH, fluorescence in-situ hybridization; HER2, human epidermal growth factor receptor 2; IHC, immunohistochemistry; LN, lymph node; NA, not applicable; NOS, not otherwise specified; Tras, trastuzumab.

over the left atrium, was determined at the earliest time point. This was compared with the corresponding time of blood sampling for %ID/l using serum gamma counting, which was then extrapolated to the blood concentration, based on the hematocrit level (Table 3). To compare the accuracy of both methods, one-way analysis of variance with Bonferroni's pairwise comparison was performed between the three methods.

Imaging was performed on a Discovery STE PET/CT scanner (General Electric, Waukesha, Wisconsin, USA). Patients underwent three scans from the top of the skull to midthigh at $\sim 1.1 \pm 0.1$, 1.8 ± 0.2, and 2.7 ± 0.5 h (mean ± SD) after injection; patients were allowed to get up between scans and urinate as needed. Images were acquired in 2D mode (typically six to seven bed positions) with 3 min per bed position. CT attenuation was performed with low-dose 80 mA CT on the initial torso scan, whereas additional scans used 10 mA to minimize the radiation dose. No oral or intravenous contrast was administered for this study.

Visual image analysis and quantification

All PET/CT images were visually analyzed by two board-certified nuclear medicine readers for any abnormal uptake, and notes were made of foci of abnormal ^{68}Ga uptake. Abnormal uptake was defined as uptake not related to expected physiological uptake and higher than adjacent or contralateral normal tissue. ^{18}F-FDG PET/CT and other imaging modalities were also available. All studies were imported to a HERMES workstation (Stockholm, Sweden) for further analysis. Volumes of interest (VOIs) were generated and SUV_{max} and SUV_{mean} values were obtained for all patients and for each time point. In addition, the total activity within the torso field of view, imaged at the three time points, was integrated on HERMES as an index of whole-body retention.

Dosimetry

For dosimetric calculations, regions of interest were drawn on four to five transverse CT slices for the left atrium, bilateral kidneys, liver, spleen, and lung, converted to VOIs, and then copied and pasted onto the corresponding sequentially acquired PET images. The mean activity concentrations in each VOI were measured in Bq/ml and overall mean values were derived for each organ. The total activity in each organ was estimated by multiplying the activity concentration by the organ mass. It was assumed that the density of all organs except that of the lung was 1 g/ml. For the lung, an average density of 0.3 g/ml was assumed.

Organ masses were taken from the OLINDA/EXM dosimetry software package (Vanderbilt University, Nashville, Tennessee, USA). Total cumulated activities in organs were estimated by integrating the time–activity curve to infinity, dividing by the injected dose, and expressing it as 'residence times' (i.e. cumulated activity per unit activity administered) for input into OLINDA/EXM. Because of the short half-life (68 min) of the radionuclide, the reduction of activity in patients as time progressed was dominated by physical decay; biological clearance was a relatively insignificant component as confirmed by integrating activity in the whole body over the three torso scans. For purposes of radiation dosimetry it was assumed that the effective whole-body residence time was 1.63 h, corresponding to physical decay, with no biological clearance.

Values of residence time were entered into OLINDA for those organs assessed by VOI analysis. For the cardiac contents and the red marrow, residence time was based on blood concentration, which was based on serum activity measurements normalized to hematocrit levels. A remainder-of-body contribution was defined as the whole-body residence time minus the sum of the individually derived values. Dose estimates were then calculated using the 57 kg 'Standard Female' phantom, except for patient 5 for whom all masses were rescaled on the basis of the ratio of actual to standard whole-body mass because of the patient's obesity.

Results

Toxicity

All injections were well tolerated. No allergic reactions were observed and no infusion had to be interrupted. No significant changes in vital signs were observed. There were no side effects or clinically detectable pharmacological effects attributable to antibody injection in any of the 15 patients. One patient was admitted for fever and abdominal pain the day after antibody infusion, but that event was attributed to chemotherapy the day before antibody infusion.

Pharmacokinetics

Biological plasma clearance curves of the antibody are summarized as the mean ± SD (Fig. 1). Compared with the radioactivity in the plasma at the initial 0.6 ± 0.1 h time sampled, at 3.1 ± 0.3 h after injection there was an average of $58.6 \pm 17\%$ of the original activity left in the plasma volume, indicating that a mean of 41.4% of the radioactivity in the plasma at the end of the infusion had left the intravascular compartment. Summary pharmacokinetic parameters of 14 of the 15 patients are shown in Table 2; one patient was excluded because of outlying data that did not fit a single or biexponential clearance. The volume of distribution of the central compartment was 4.09 ± 1.51 l, which was significantly greater than the plasma volume (2.34 ± 0.12 l) ($P < 0.001$, paired t-test).

To determine the accuracy of ^{68}Ga PET imaging for quantitation, the concentration in the serum was extrapolated to that in the blood, based on the patients' hematocrit level, and showed a mean concentration of

Fig. 1

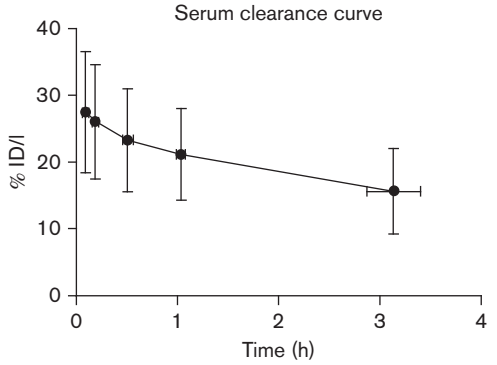

The average biological serum clearance curve for ^{68}Ga-DOTA-F(ab′)$_2$-trastuzumab from all 15 patients is plotted with SDs in both the time and %ID/l serum axis. ^{68}Ga-DOTA-F(ab′)$_2$-trastuzumab, ^{68}Ga-1,4,7,10-tetraazacyclododecane-*N*,*N*′,*N*″,*N*‴-tetraacetic acid (DOTA)-F(ab′)$_2$-trastuzumab.

Table 2 Pharmacokinetic properties

Parameters	Value ($n=14$)
C_0 (%ID/l)	27.2±8.6
$T_{½}$ (h)	3.6±0.9
AUC to last time point (%ID × h/l)	60.4±18.1
AUC fit to infinity (%ID × h/l)	143.9±59.2
Clearance (l/h)	0.82±0.38
Volume distribution central compartment (l)	4.09±1.51

AUC, area under the curve; C_0, concentration at time 0.

Table 3 Comparison of concentration of ^{68}Ga-DOTA-F(ab′)$_2$-trastuzumab in blood volume determined from gamma counter measurements of serum or from SUV_{max} and SUV_{mean} from PET images

Patient ID	%ID/l[a] counter	%ID/l (SUV_{max})	%ID/l (SUV_{mean})	$\triangle t$[b] (h)
1	17.56	12.77	6.95	0.31
2	38.89	29.67	17.47	0.22
3	31.16	29.88	24.02	0.17
4	21.29	24.51	17.13	0.03
5	28.06	26.12	17.80	0.15
6	20.40	25.51	16.97	0.21
8	26.20	22.28	14.42	0.08
9	21.15	25.14	14.41	0.03
10	22.04	35.76	15.83	0.03
11	27.90	32.73	34.16	0.08
12	21.91	24.90	15.85	0.14
13	18.46	30.66	18.58	0.10
14	29.24	34.37	21.79	0.01
16	27.30	35.93	21.11	0.10
17	21.71	24.15	12.05	0.05

^{68}Ga-DOTA-F(ab′)$_2$-trastuzumab, ^{68}Ga-1,4,7,10-tetraazacyclododecane-*N*,*N*′,*N*″,*N*‴-tetraacetic acid (DOTA)-F(ab′)$_2$-trastuzumab; SUV, standardized uptake value.
[a]Serum %ID/l from gamma counter data was converted to %ID/l of blood based on hematocrit level.
[b]Time difference between gamma counter measurements and PET scan.

24.9±5.8%ID/l, which was not significantly different than the 27.6±6.1%ID/l determined from SUV_{max} ($P=0.61$). In contrast, the SUV_{mean} underestimated the concentration in blood (17.9±6.1%ID/l; $P=0.007$) (Table 3).

Biodistribution and imaging

PET images showed significant blood pool retention with corresponding decrease over time (Fig. 2). The kidneys had the highest concentration with a slight increase over time. The liver also had prominent activity with a significant amount accounted for by the blood pool. Although liver activity was stable over time, the liver to blood pool ratio increased, indicating slight concentration (Fig. 3). This relatively intense liver uptake in patients might limit the ability to evaluate hepatic metastases. Although with our method we would not have expected a significant amount of colloid formation or aggregate formation, we have retested the DOTA-F(ab′)$_2$ during ^{68}Ga radiolabeling for colloid using an instant thin-layer chromatography method and none were found. We have also performed a size exclusion high-performance liquid chromatography analysis of the chelated antibody fragment before and after radiolabeling and have found only a small amount of aggregate, which will not explain the concentration of ^{68}Ga observed in the liver (data not shown).

The visual analysis of the lesions is given in Table 1. In all, seven of 15 (47%) patients had HER2-negative breast cancer on histological analysis and did not show any tumor localization of ^{68}Ga (Table 1). Eight (53%) patients were HER2 positive and three among them had ongoing therapy with trastuzumab at the time of scanning. One of the patients with HER2-positive breast cancer was trastuzumab naive, whereas all others had received prior treatment. All patients with HER2-positive disease had undergone recent ^{18}F-FDG scans and all had ^{18}F-FDG-avid disease. All seven patients with HER2-negative breast cancer also had ^{18}F-FDG-positive disease. Only seven ^{18}F-FDG-avid lesions showed appreciable ^{68}Ga-DOTA-F(ab′)$_2$-trastuzumab uptake in a total of four patients. As an example, in patient 1, a lytic skull lesion showed ^{68}Ga-DOTA-F(ab′)$_2$-trastuzumab uptake (SUV = 3.42) (Fig. 4). In patient 2, who had multiple bilateral parenchymal lung nodules consistent with metastases, only minimal ^{68}Ga-DOTA-F(ab′)$_2$-trastuzumab uptake was noted (SUV range 2.40–3.79) (Fig. 5).

Dosimetry results

The mean absorbed organ doses obtained from OLINDA are shown in Table 4. The largest mean dose was to the kidneys, 0.383 cGy/37 MBq. The mean dose to the liver and heart was 0.359 cGy/37 MBq and 0.278 cGy/37 MBq, respectively.

Discussion

Breast cancer is a significant health problem in the USA and worldwide [16]. HER2 overexpression was associated with worse outcomes before the advent of targeted

Fig. 2

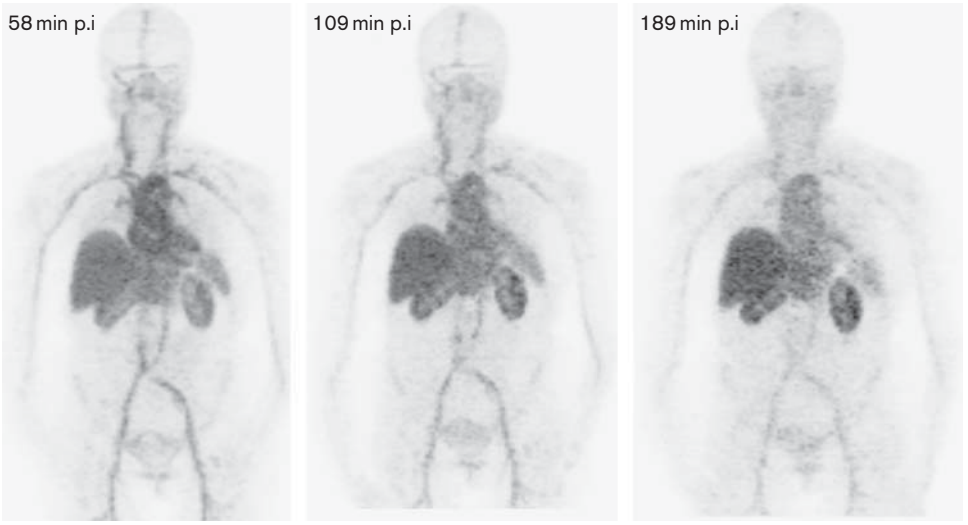

Serial MIP images (patient 6) displayed at the same relative intensity. Although a slight decrease in blood pool is present, blood pool activity dominates the distribution. At 58, 109, and 189 min the blood pool has SUV_{max} of 16.9, 13.6, and 9.8, respectively. There is slight increased uptake over time in the liver and kidneys. The patient had HER2-positive disease and was receiving lapatinib. Tumors in the left adrenal, hilar nodes, and bones were not visualized on Ga-PET. HER2, human epidermal growth factor receptor 2; MIP, maximum intensity projection; p.i, postinjection; SUV, standardized uptake value.

Fig. 3

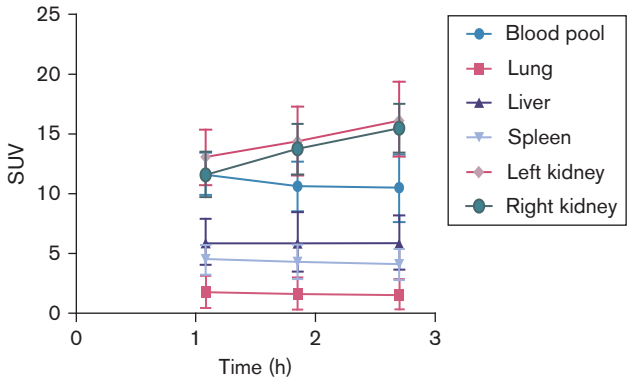

Mean SUV body weight organ values obtained at the three imaging times are plotted. For small structures such as blood pool and kidney, SUV_{max} was utilized, whereas for all other organs SUV_{mean} was used. SUV, standardized uptake value.

agents [17,18]. HER2 is overexpressed in breast cancer and in a variety of other tumors including gastric cancer, where trastuzumab has also been shown to be of benefit. Despite these advances, response rates to single-agent trastuzumab are modest (12–26%) [19–21]. Moreover, resistance to trastuzumab may present *de novo* and it eventually develops in the majority of cases of metastatic disease. This has motivated the search for and development of other anti-HER2 therapeutic strategies, including novel antibodies (e.g. pertuzumab), antibody conjugates (e.g. ado-trastuzumab-emtamsine), small-molecule tyrosine kinase inhibitors of HER2 (e.g. lapatinib, neratinib), and novel agents like HSP90 inhibitors (e.g. 17-AAG), which induce HER2 degradation [3]. One potential obstacle in the optimal development of these anti-HER2 therapies is the inability to directly assess the effects of these drugs on their intended targets in patients. Our group had previously shown that ^{68}Ga-DOTA-F(ab′)$_2$-trastuzumab is a better predictor of tumor response compared with ^{18}F-FDG PET in tumor xenografts [22]. Other groups have found in preclinical models that radiolabeled trastuzumab may be used to measure target effects [8,12,23]. Furthermore, we have seen evidence of this in the clinic, where the ability to target HER2 may help patient management by predicting which patients are likely to respond to therapy or to develop toxicity from therapy [6,11].

The results we observed in 15 patients showed that most ^{18}F-FDG-avid lesions did not show significant ^{68}Ga-DOTA-F(ab′)$_2$-trastuzumab uptake. The study group consisted of both trastuzumab-naive patients ($n = 8$), patients who had received prior therapy with this agent ($n = 7$), and those in whom it was ongoing at the time of imaging ($n = 3$). One explanation for our findings is that high circulating levels of trastuzumab may compete and interfere with tumor targeting by ^{68}Ga-DOTA-F(ab′)$_2$-trastuzumab. One limitation may be the optimal amount of F(ab′)$_2$-trastuzumab mass; Dijkers *et al.* [24] demonstrated that 50 mg of antibody had to be used to obtain optimal results in patients not receiving trastuzumab in whom 10 mg was suboptimal. In our study group the same amount of 4.5–5.5 mg F(ab′)$_2$-trastuzumab fragments was

Fig. 4

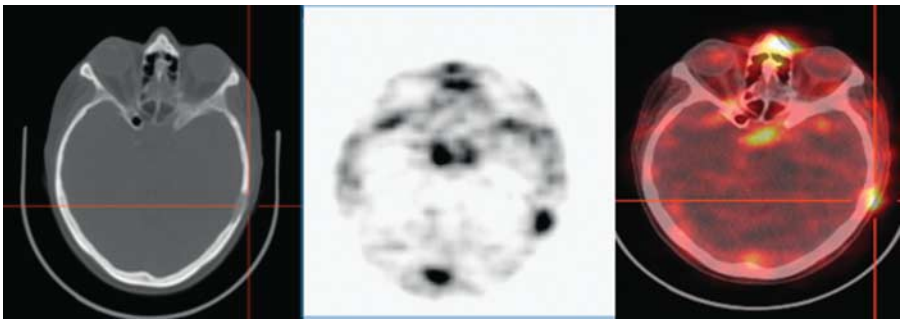

Lytic lesion in the left calvarium with ^{68}Ga-DOTA-F(ab′)$_2$-trastuzumab uptake (patient 1). ^{68}Ga-DOTA-F(ab′)$_2$-trastuzumab, ^{68}Ga-1,4,7,10-tetraazacyclododecane-*N*,*N*′,*N*″,*N*‴-tetraacetic acid (DOTA)-F(ab′)$_2$-trastuzumab.

Fig. 5

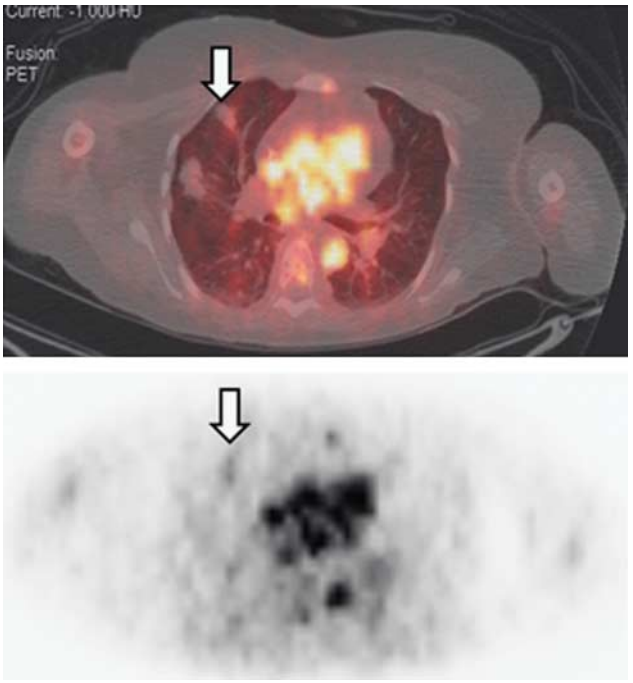

In patient 2, fused images obtained at ~1 h show mild ^{68}Ga-DOTA-F(ab′)$_2$-trastuzumab uptake in a lung metastasis. ^{68}Ga-DOTA-F(ab′)$_2$-trastuzumab, ^{68}Ga-1,4,7,10-tetraazacyclododecane-*N*,*N*′,*N*″,*N*‴-tetraacetic acid (DOTA)-F(ab′)$_2$-trastuzumab.

used both in patients receiving trastuzumab treatment and those who were not.

It is well known that intact antibodies take time to extravasate and localize in tumor tissues. This is the reason that radioisotopes used to label intact antibodies such as ^{111}In, ^{131}I, ^{89}Zr, and ^{124}I typically have half-lives that number in days. In our studies we used F(ab′)$_2$, which typically has faster kinetics than IgG, with some reports in the literature showing five-fold longer half-life for the IgG form compared with F(ab′)$_2$ fragments [25]. In our animal studies, good targeting was obtained within the relevant time frame for ^{68}Ga short half-life. In the current clinical study the estimated half-life was short (3.6±0.9 h) and, as a group, ~66% of the injected dose had moved out of the vascular component at the last imaging point and would have been expected to be adequate for imaging. Nonetheless, radionuclides with a slightly longer half-life that would allow for imaging at 6–24 h may be more useful, such as ^{64}Cu [8,26,27]. Several groups have used affibodies that are antibody mimetic compounds to target HER2, taking advantage of their smaller size and much faster biological clearance to label these with ^{68}Ga [28–30]. Using affibodies labeled with ^{68}Ga or ^{111}In, Baum *et al.* [28] reported visualization of most ^{18}F-FDG-avid lesions in three patients with breast cancer.

Our study showed relatively fast clearance of the antibody from the intravascular compartment. At the very first time point, ~5 min after the end of infusion, the plasma activity accounted only for approximately a mean of 66.4% of the injected activity, with an additional decrease to ~38.9% of the injected activity in the plasma at 3 h. This is partly likely due to the smaller size of the F(ab′)$_2$ and lack of Fc component compared with intact IgG. Nonetheless, the possibility of some damage with faster clearance cannot be completely excluded. Although we did not routinely perform high-performance liquid chromatography analysis of the serum because of the challenges of the short half-life, in one patient (data not shown) serial samples did not show breakdown to smaller fragments. Other studies with F(ab′)$_2$ fragments do demonstrate biexponential clearance with a shorter half-life of F(ab′)$_2$ compared with IgG. For example, Massuger *et al.* [31] reported a fast component of 6.1±1.1 h and a slow component of 17.9±6.5 h. Kalofonos *et al.* [32] reported a fast component of 2.5±1.3 h and a slow component of 42±4.5 h for ^{111}In-labeled HMFG F(ab′)$_2$ fragments. Brouwers and colleagues observed that radioiodinated

cG250-F(ab′)$_2$ fragments were characterized by a rapid distribution phase, with a half-life ranging from 4.1 to 6.3 h (mean: 4.8 h), and a slower elimination phase, with a half-life ranging from 25.8 to 34.1 h (mean: 29.0 h). At 96 h after injection only 20% of the injected dose was still present in the body, compared with 60%ID for intact cG250, demonstrating faster clearance of F(ab′)$_2$ fragments [33]. De Bree *et al.* [34] reported a mean elimination half-life of 6.6 ± 2.6 and 54.1 ± 24.3 h for E48 IgG, whereas the E48 F(ab′)$_2$ fragment showed an elimination half-life of 2.3 ± 0.4 and 19.9 ± 4.6 h in a group of patients with head and neck cancer. Because of limited data points in our patients, biexponential clearance could not be adequately fitted in most patients, and thus some of the observed pharmacokinetic differences may be technical.

Our biodistribution and dosimetry study also demonstrated that the mouse dosimetry that was used as a starting point for dosimetry estimates was within 57.32% (average) of the actual dosimetry calculated (Table 4). Excluding heart wall, liver, red marrow, spleen, and bladder wall, the estimates were within 22.65%. For effective dose and effective dose equivalent, the estimated values were off only by 2.9 and 14.8%, respectively.

The immunoreactivity assay result of ^{68}Ga trastuzumab was lower than that of most of our other antibodies and may reflect some alteration in the immunoreactivity of the antibody during processing. Nonetheless, our animal biodistribution studies showed good targeting of tumor xenografts with the same batch of reagent [22]. This lower immunoreactivity may represent an underestimation due to affinity changes.

Although recent studies with ^{89}Zr trastuzumab have shown promising results [24], the long half-life imposes limitations related to imaging performed at 3–5 days after tracer administration, including dosimetry, availability of radionuclide, and patient convenience issues. Searching for faster HER2 imaging paradigms would be useful from a patient's convenience point of view and would also allow the performance of short-term and/or repeated assessment after an intervention.

Table 4 Mean absorbed doses for all 15 patients versus estimated values from the murine dosimetry(cGy/37 MBq)

Target organ	Actual[a] (cGy/37 MBq)	Estimated (cGy/37 MBq)
Adrenals	0.064	0.056
Brain	0.036	0.045
Breasts	0.042	0.044
Gallbladder wall	0.066	0.058
LLI wall	0.044	0.080
Small intestine	0.046	0.093
Stomach wall	0.050	0.084
ULI wall	0.049	0.069
Heart wall	0.278	0.109
Kidneys	0.383	0.418
Liver	0.359	0.096
Lungs	0.225	0.167
Muscle	0.042	0.041
Ovaries	0.045	0.060
Pancreas	0.061	0.057
Red marrow	0.094	0.041
Osteogenic cells	0.113	0.068
Skin	0.035	0.040
Spleen	0.29	0.074
Thymus	0.051	0.049
Thyroid	0.039	0.046
Urinary bladder wall	0.038	0.726
Uterus	0.044	0.070
Total body	0.060	0.062
Effective dose equivalent (cSv/37 MBq)	0.140	0.136
Effective dose (cSv/37 MBq)	0.092	0.108

LLI, lower large intestine; ULI, upper large intestine.
[a]Mean of 15 patients.

Conclusion

This pilot study showed the safety of administration of ^{68}Ga-DOTA-F(ab′)$_2$-trastuzumab in patients with breast cancer and determined that radiation dosimetry and pharmacokinetics were favorable. Although minimal or no tumor uptake of the radiolabeled antibody was seen in most cases, patient selection, immunoreactivity, and mass of the antibody may have been suboptimal. To determine the utility of ^{68}Ga-DOTA-F(ab′)$_2$-trastuzumab to image sites of disease, an ideal future study involving HER2-positive patients naive for trastuzumab, larger administered mass quantity with a high immunoreactivity fraction of ^{68}Ga-DOTA-F(ab′)$_2$-trastuzumab, and histological correlation of HER2 positivity in the tissue and PET positivity is needed.

Acknowledgements

This study was funded by ICMIC P50, Norton Breast SPORE, Ludwig Center for Cancer Immunotherapy.

Conflicts of interest

There are no conflicts of interest.

References

1 Slamon DJ, Clark GM, Wong SG, Levin WJ, Ullrich A, Mcguire WL. Human-breast cancer – correlation of relapse and survival with amplification of the HER-2 neu oncogene. *Science* 1987; **235**:177–182.
2 Hudis CA. Trastuzumab – mechanism of action and use in clinical practice. *N Engl J Med* 2007; **357**:39–51.
3 Arteaga CL, Baselga J. Impact of genomics on personalized cancer medicine. *Clin Cancer Res* 2012; **18**:612–618.
4 Yin W, Jiang Y, Shen Z, Shao Z, Lu J. Trastuzumab in the adjuvant treatment of HER2-positive early breast cancer patients: a meta-analysis of published randomized controlled trials. *Plos One* 2011; **6**:e21030.
5 Sauter G, Lee J, Bartlett JM, Slamon DJ, Press MF. Guidelines for human epidermal growth factor receptor 2 testing: biologic and methodologic considerations. *J Clin Oncol* 2009; **27**:1323–1333.
6 Behr TM, Behe M, Wormann B. Trastuzumab and breast cancer. *N Engl J Med* 2001; **345**:995–996.
7 Perik PJ, Lub-De Hooge MN, Gietema JA, van der Graaf WT, de Korte MA, Jonkman S, *et al.* Indium-111-labeled trastuzumab scintigraphy in patients with human epidermal growth factor receptor 2-positive metastatic breast cancer. *J Clin Oncol* 2006; **24**:2276–2282.
8 Niu G, Li Z, Cao Q, Chen X. Monitoring therapeutic response of human ovarian cancer to 17-DMAG by noninvasive PET imaging with (64)Cu-DOTA-trastuzumab. *Eur J Nucl Med Mol Imaging* 2009; **36**:1510–1519.
9 Moreau M, Raguin O, Vrigneaud JM, Collin B, Bernhard C, Tizon X, *et al.* DOTAGA-trastuzumab. A new antibody conjugate targeting HER2/neu antigen for diagnostic purposes. *Bioconjug Chem* 2012; **9**:1181–1188.

10 Dijkers EC, Kosterink JG, Rademaker AP, Perk LR, van Dongen GA, Bart J, *et al*. Development and characterization of clinical-grade ^{89}Zr-trastuzumab for HER2/neu immunoPET imaging. *J Nucl Med* 2009; **50**:974–981.

11 Gaykema SB, Brouwers AH, Hovenga S, Lub-de Hooge MN, de Vries EG, Schroder CP. Zirconium-89-trastuzumab positron emission tomography as a tool to solve a clinical dilemma in a patient with breast cancer. *J Clin Oncol* 2012; **30**:e74–e75.

12 Holland JP, Caldas-Lopes E, Divilov V, Longo VA, Taldone T, Zatorska D, *et al*. Measuring the pharmacodynamic effects of a novel Hsp90 inhibitor on HER2/neu expression in mice using Zr-DFO-trastuzumab. *Plos One* 2010; **5**:e8859.

13 Smith-Jones PM, Solit DB, Akhurst T, Afroze F, Rosen N, Larson SM. Imaging the pharmacodynamics of HER2 degradation in response to Hsp90 inhibitors. *Nat Biotechnol* 2004; **22**:701–706.

14 Smith-Jones PM, Solit DB. Generation of DOTA-conjugated antibody fragments for radioimmunoimaging. *Methods Enzymol* 2004; **386**: 262–275.

15 Lindmo T, Boven E, Cuttitta F, Fedorko J, Bunn PA. Determination of the immunoreactive fraction of radiolabeled monoclonal-antibodies by linear extrapolation to binding at infinite antigen excess. *J Immunol Methods* 1984; **72**:77–89.

16 Siegel R, Naishadham D, Jemal A. Cancer statistics, 2012. *CA Cancer J Clin* 2012; **62**:10–29.

17 Slamon DJ, Leyland-Jones B, Shak S, Fuchs H, Paton V, Bajamonde A, *et al*. Use of chemotherapy plus a monoclonal antibody against HER2 for metastatic breast cancer that overexpresses HER2. *N Engl J Med* 2001; **344**:783–792.

18 Dawood S, Giordano SH. Improved prognosis by trastuzumab of women with HER2-positive breast cancer compared with those with HER2-negative disease – reply to G. Ferretti *et al. J Clin Oncol* 2010; **28**:E338–E339.

19 Cobleigh M. Herceptin (R) is active as a single agent in women with metastatic breast cancer overexpressing HER2. *Eur J Cancer* 1999; **35**:S316.

20 Cobleigh MA, Vogel CL, Tripathy D, Robert NJ, Scholl S, Fehrenbacher L, *et al*. Multinational study of the efficacy and safety of humanized anti-HER2 monoclonal antibody in women who have HER2-overexpressing metastatic breast cancer that has progressed after chemotherapy for metastatic disease. *J Clin Oncol* 1999; **17**:2639–2648.

21 Vogel CL, Cobleigh MA, Tripathy D, Gutheil JC, Harris LN, Fehrenbacher L, *et al*. Efficacy and safety of trastuzumab as a single agent in first-line treatment of HER2-overexpressing metastatic breast cancer. *J Clin Oncol* 2002; **20**:719–726.

22 Smith-Jones PM, Solit D, Afroze F, Rosen N, Larson SM. Early tumor response to Hsp90 therapy using HER2 PET: comparison with F-18-FDG PET. *J Nucl Med* 2006; **47**:793–796.

23 Munnink THO, de Korte MA, Nagengast WB, Timmer-Bosscha H, Schroder CP, de Jong JR, *et al*. Zr-89-trastuzumab PET visualises HER2 downregulation by the HSP90 inhibitor NVP-AUY922 in a human tumour xenograft. *Eur J Cancer* 2010; **46**:678–684.

24 Dijkers EC, Oude Munnink TH, Kosterink JG, Brouwers AH, Jager PL, de Jong JR, *et al*. Biodistribution of ^{89}Zr-trastuzumab and PET imaging of HER2-positive lesions in patients with metastatic breast cancer. *Clin Pharmacol Ther* 2010; **87**:586–592.

25 Spiridon CI, Guinn S, Vitetta ES. A comparison of the in vitro and in vivo activities of IgG and F(ab′)$_2$ fragments of a mixture of three monoclonal anti-Her-2 antibodies. *Clin Cancer Res* 2004; **10**:3542–3551.

26 Olafsen T, Kenanova VE, Sundaresan G, Anderson AL, Crow D, Yazaki PJ, *et al*. Optimizing radiolabeled engineered anti-p185HER2 antibody fragments for in vivo imaging. *Cancer Res* 2005; **65**:5907–5916.

27 Ren G, Webster JM, Liu Z, Zhang R, Miao Z, Liu H, *et al*. In vivo targeting of HER2-positive tumor using 2-helix affibody molecules. *Amino acids* 2012; **43**:405–413.

28 Baum RP, Prasad V, Muller D, Schuchardt C, Orlova A, Wennborg A, *et al*. Molecular imaging of HER2-expressing malignant tumors in breast cancer patients using synthetic ^{111}In- or ^{68}Ga-labeled affibody molecules. *J Nucl Med* 2010; **51**:892–897.

29 Kramer-Marek G, Shenoy N, Seidel J, Griffiths GL, Choyke P, Capala J. ^{68}Ga-DOTA-affibody molecule for in vivo assessment of HER2/neu expression with PET. *Eur J Nucl Med Mol Imaging* 2011; **38**:1967–1976.

30 Tolmachev V, Velikyan I, Sandstrom M, Orlova A. A. HER2-binding affibody molecule labelled with ^{68}Ga for PET imaging: direct in vivo comparison with the ^{111}In-labelled analogue. *Eur J Nucl Med Mol Imaging* 2010; **37**: 1356–1367.

31 Massuger L, Claessens R, Kenemans P, Verheijen RHM, Boerman OC, Meeuwis APW, *et al*. Kinetics and biodistribution in relation to tumor-detection with In-111 labeled OV-TL 3 F(ab′)$_2$ in patients with ovarian-cancer. *Nucl Med Commun* 1991; **12**:593–609.

32 Kalofonos HP, Sivolapenko GB, Courtenayluck NS, Snook DE, Hooker GR, Winter R, *et al*. Antibody guided targeting of non-small cell lung-cancer using In-111-labeled HMFG1 F(ab′)$_2$ fragments. *Cancer Res* 1988; **48**:1977–1984.

33 Brouwers A, Mulders P, Oosterwijk E, Buijs W, Corstens F, Boerman O, *et al*. Pharmacokinetics and tumor targeting of I-131-labeled F(ab′)(2) fragments of the chimeric monoclonal antibody G250: preclinical and clinical pilot studies. *Cancer Biother Radiopharm* 2004; **19**: 466–477.

34 De Bree R, Roos JC, Quak JJ, den Hollander W, Wilhelm AJ, van Lingen A, *et al*. Biodistribution of radiolabeled monoclonal antibody E48 IgG and F(ab′)$_2$ in patients with head and neck cancer. *Clin Cancer Res* 1995; **1**:277–286.